ACS Sustainable Chemistry & Engineering

Letter

pubs.acs.org/journal/ascecg

Low-Cost CZTSSe Solar Cells Fabricated with Low Band Gap CZTSe Nanocrystals, Environmentally Friendly Binder, and Nonvacuum Processes

Chih-Liang Wang and Arumugam Manthiram*

Materials Science and Engineering Program, The University of Texas at Austin, Austin, Texas 78712, United States

Supporting Information

ABSTRACT: High quality $Cu_2ZnSn(SSe)_4$ (CZTSSe) for solar cells can be fabricated with Cu_2ZnSnS_4 (CZTS) nanocrystals, followed by a selenization process. However, the use of toxic and environmentally unfriendly solvents such as toluene or hexanethiol to disperse the nanocrystals and the use of the harsh selenization process to promote the grain growth are not environmentally benign. We present here an environmentally friendly, sustainable, and scalable route to fabricate CZTSSe with $Cu_2ZnSnSe_4$ (CTZSe) nanocrystals by a sulfurization process. The CZTSSe film has been doped with S to optimize the device performance, exhibiting an enhancement in the open-circuit voltage (V_{oc}) and short circuit current density (J_{sc}). In addition, by developing a robust precursor film with the addition of ethyl cellulose, the loss of Sn associated with the conversion of CZTSe to CZTSSe during the grain growth process has been mitigated, leading to an increase in the conversion efficiency compared to that of the precursor film without using ethyl cellulose. Such an improvement can provide insight into the grain growth of CZTSSe during the sulfurization process and thereby enhance the feasibility of sustainable high efficiency CZTSSe solar devices.

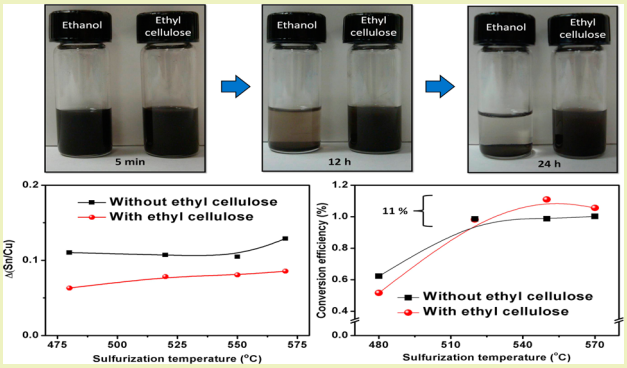

KEYWORDS: *Solar cells, Superstrate-type substrate, CZTSSe, Sulfurization, Sn loss, Ethyl cellulose*

INTRODUCTION

Colloidal semiconductor nanocrystals are one of the promising solutions to achieve the ultimate goal of low-cost high-efficiency solar cells due to the advantages of efficient utilization of materials, excellent capability for precisely controlled compositions, and large-scale manufacturing processes.[1] Recently, successful application of semiconductor nanocrystals such as CdTe,[2] CIGS,[3] and PbS[4] to photovoltaic devices has been demonstrated to ensure their potential. However, with the targeted deployment of solar cells reaching the terawatt scale, those materials adopting the rare or environmentally unfriendly elements would become a crucial issue.[5] The environmentally benign and earth-abundant kesterite-related Cu_2ZnSnS_4 (CZTS), $Cu_2ZnSn(S_xSe_{1-x})_4$ (CZTSSe), and $Cu_2ZnSnSe_4$ (CZTSe) materials with high absorption coefficients become promising absorbent candidates for the next generation solar cells to meet the terawatt-scale solar demand.[6] Recently, many efforts have been made with the syntheses of CZTS,[7] CZTSe, and CZTSSe[8] nanocrystals. However, it is challenging to make high-quality films to promote the transport of electrons and holes for producing high-efficiency pn junction solar devices.

An efficiency of 0.8% was demonstrated using CZTS nanocrystals followed by a selenization process, and such an approach has become a prevailing route for making CZTSSe solar cells.[9] With further improvements in coating the film by adopting a hexanethiol solvent, a higher efficiency of 6.73% has been achieved by the same group.[10] However, the utilization of toxic and unfriendly solvents such as toluene or hexanethiol to disperse the nanocrystals is not environmental friendly. Unfortunately, only a few studies have focused on green and sustainable binders for preparing the CZTSSe nanocrystal-based ink. On the other hand, the typical selenization process by inefficiently using a large amount of rare Se element (with only 0.05 ppm in the earth's crust) during heat treatment makes it challenging to meet the terawatt-scale demand of solar cells.[11] In addition, the active Se during heat treatment not only easily creates an unwanted layer of $MoSe_2$ at the interface but also causes undesirable effects on the device performance, leading to difficulties in controlling the manufacturing process.[12] In contrast to the traditional route for CZTSSe involving inefficient and harsh chemical reaction processes associated with Se, an alternative route for CZTSSe involving the sulfurization of the fabricated precursor CZTSe nanocrystals with the abundant and mild S element could enhance the commercial viability of CZTSSe solar cells. Unfortunately, only a few studies have focused on this route.

Received: September 11, 2013
Revised: December 26, 2013
Published: January 19, 2014

   dx.doi.org/10.1021/sc400465m | ACS Sustainable Chem. Eng. 2014, 2, 561−568

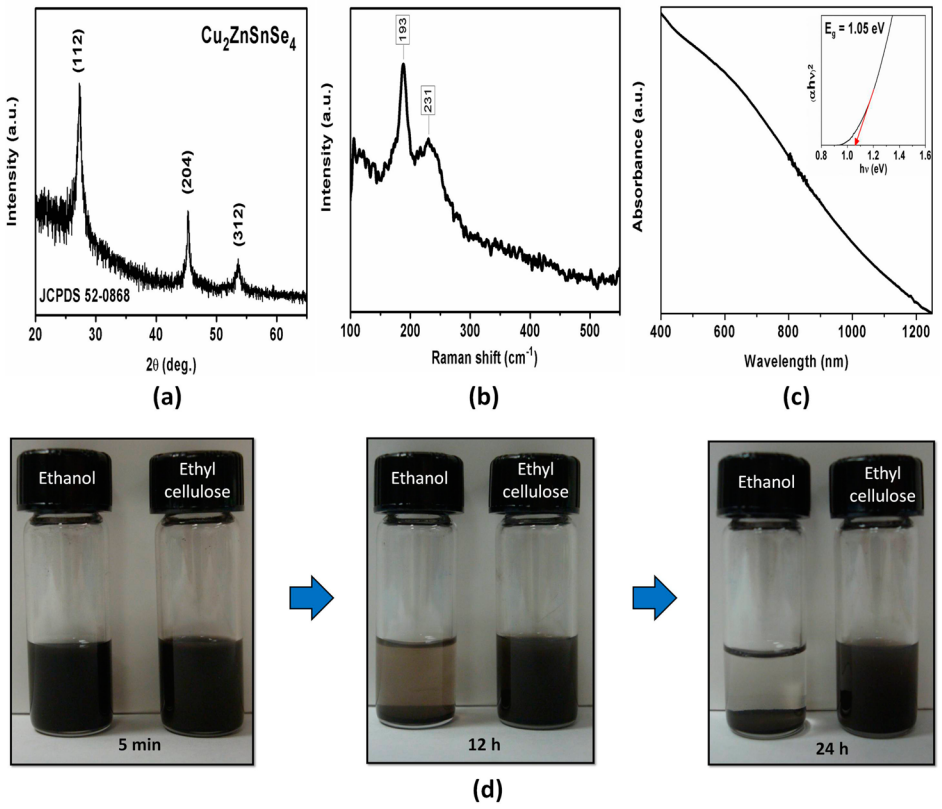

Figure 1. (a) XRD patterns of as-synthesized CZTSe nanocrystals, (b) Raman spectroscopic analyses of as-synthesized CZTSe nanocrystals, (c) UV−vis absorption spectrum of as-synthesized CZTSe nanocrystals, and (d) color of the vial containing the CZTSe nanocrystals dispersed in ethanol with and without ethyl cellulose after the standing for a period of 5 min, 12 h, and 24 h. The inset in (c) shows a band gap of 1.05 eV for the as-synthesized CZTSe nanocrystals, determined by a plot of $(\alpha h\upsilon)^2$ as a function of $h\upsilon$.

Accordingly, we demonstrate here a new route to make the CZTSSe films by using the low band gap CZTSe nanocrystals, synthesized by a hot injection approach, followed by a sulfurization process. The effect of S doping into CZTSe nanocrystals during heat treatment is also investigated by varying the sulfurization temperature from 480 to 570 °C. Furthermore, ethyl cellulose, which can replace the toxic and unfriendly solvent of toluene or hexanethiol, is used as a binder in the film preparation process with CZTSe nanocrystals. In order to investigate the role of ethyl cellulose in the evolution of nanocrystals into films, a low-cost superstrate-type substrate is adopted to evaluate the conversion efficiency.

EXPERIMENTAL METHOD

Synthesis of $Cu_2ZnSnSe_4$ Nanocrystals. The CZTSe nanocrystals were produced by a hot injection approach. Cationic precursors of Cu, Zn, and Sn were selected from copper(II) acetylacetonate $[Cu(acac)_2]$, zinc acetate $[Zn(O_2CCH_3)_2]$, and tin(II) chloride dihydrate $[SnCl_2.2H_2O]$, respectively. In a typical synthesis, a mixed solution of 1.61 mmol of copper(II) acetylacetonate, 1.3 mmol of zinc acetate, and 1.0 mmol of tin(II) chloride dehydrate with 30 mL of oleylamine was heated first. A 10 mL of oleylamine solution with elemental Se was injected into the mixed solution at 200 °C. Then, the solution mixture was heated to 250 °C with a holding time of 1 h. After cooling to room temperature, the product was precipitated into methanol and washed with isopropyl alcohol/hexane three times to remove the residual oleylamine.

Fabrication of Solar Devices. The conversion efficiency of the solar devices was examined with a low-cost and $Mo(S,Se)_2$-free superstrate-type substrate of $CdS/TiO_2/ITO$/soda-lime glass with a layer (30 nm) of anatase TiO_2 synthesized by a sol−gel method at 450 °C and a buffer layer (100 nm) of CdS prepared by a chemical bath deposition (CBD) method at 65 °C on a commercial ITO substrate.[13] No antireflectance coating of MgF_2 was used. A gold electrode prepared by a thermal evaporator was used to define an active area of 0.1 cm^2. Two inks were prepared for the spin-coating process. Although the nanocrystals could be well dispersed in a nonpolar solvent, the toxicity or high volatility of most of the nonpolar solvents make it challenging to prepare a scalable and uniform film with the spin-coating process. Therefore, the environmentally friendly and safe solvent ethanol with relatively low volatility was chosen for the spin-coating process. Besides, in order to investigate the effect of the binder on the ink, ethyl cellulose with more than 46−48% ethoxyl groups that freely dissolve in ethanol was used. The first ink was prepared by dispersing 10 mg of CZTSe in 0.8 mL of ethanol by ultrasonication for 20 min. The other ink was prepared by dispersing 10 mg of CZTSe in a premixed solution of 0.8 mL of ethanol with 0.3 mg of ethyl cellulose by ultrasonication for 20 min. After spin-coating onto the superstrated-type substrate, the as-prepared film (ink without ethyl cellulose) and the composite film (ink with ethyl cellulose) were treated by a sulfurization process from 480 to 570 °C for 45 min. The sulfurizaiton process was performed by placing the samples in a graphite box with sulfur powder under an argon flow. Once the tubular furnace was preheated to a desirable temperature, the whole graphite box was immediately moved to the heating region to provide a fast ramping rate and mitigate the effect of potential diffusion at the interface. An etching process with dilute HCl (hydrochloric acid) solution was applied before thermally depositing the gold back contact.[14]

Characterization of Materials. The CZTSe sample was characterized with a Philips X-ray diffractometer (XRD) with Cu Kα radiation. The band gap of CZTSe was determined by a Cary 5000 UV−vis−NIR equipment. The CZTSe nanocrystals dispersed in hexane were used for UV−vis absorption measurements to avoid the extra signals from those dispersed in a premixed solution of ethanol

dx.doi.org/10.1021/sc400465m | ACS Sustainable Chem. Eng. 2014, 2, 561−568

and ethyl cellulose. The Raman spectra were acquired with a Renishaw inVia Raman microscope using 532 nm laser excitation at a 50X objective. The in-plane and cross-sectional images were collected with a FEI Quanta 650 scanning electron microscope (SEM). The compositional analyses collected with energy-dispersive X-ray spectroscopy (EDS) were carried out with a JOEL5610 SEM. Thermogravimetric analysis (TGA) was performed with a Perkin–Elmer TGA 7 with 5 °C per minute heating rate under a flow of argon. The current density–voltage (J–V) characteristics under an air mass of 1.5 global (AM 1.5 G) conditions with a solar simulator using a 100 mW cm^{-2} light illumination were measured with Keithley 2400 equipment. The conversion efficiencies of all solar cells based on a superatrate-type substrate were assessed with the light illuminating into the ITO side of the substrate. Silver paste was used to reduce the contact resistance between ITO and the wire.

RESULTS AND DISCUSSION

Figure 1(a) shows the X-ray diffraction (XRD) pattern of the as-synthesized CZTSe nanocrystals, which matches well with all the diffraction peaks in the Joint Committee on Powder Diffraction Standards (JCPDS) card 52-0868. The CZTSe unit cell has lattice constants of a = 5.64 Å and c = 11.20 Å with a volume of 356.26 $Å^3$, which is larger than the 319.50 $Å^3$ volume of CZTS because of the larger radius of Se (0.198 nm) compared to that of S (0.184 nm). According to the Debye–Scherrer analysis, the as-synthesized CZTSe nanocrystals have an average crystallite size of 20 nm. Raman spectroscopic analysis in Figure 1(b) also indicates that the as-synthesized nanocrystals can be identified with the main peaks of 196 and 231 cm^{-1} in the CZTSe crystallite structure. A small deviation between 193 and 196 cm^{-1} may be attributed to uneven surface scattering. Furthermore, Figure 1(c) shows the absorbance of as-synthesized CZTSe nanocrystals as a function of the wavelength. It can be found that the CZTSe nanocrystals possess a low energy band gap of 1.05 eV, as determined from the UV–vis absorption spectrum, shown in the upper inset of Figure 1(c), which is consistent with the previous literature.[15]

These analyses show that a single phase of CZTSe nanocrystals with low energy band of 1.05 eV has been synthesized by the hot injection approach. In addition, in order to compensate the potential loss of Sn during heat treatment, the as-synthesized CZTSe nanocrystals with cation ratios of Zn/Sn = 0.99 and Cu/(Zn+Sn) = 0.72, analyzed by EDS, is suitable for fabricating Cu-poor and Zn-rich CZTSSe solar cells. On the other hand, the effect of ethyl cellulose on CZTSe nanocrystals was evaluated by dispersing the nanocrystals in ethanol with and without ethyl cellulose as shown in Figure 1(d). After a period of 12 h, the middle segment in Figure 1(d) shows that some of the nanoparticles dispersed in ethanol have settled at the bottom compared to that dispersed in ethanol with ethyl cellulose. After a period of 24 h, the color of the supernatant liquid in the vial with the nanoparticles dispersed in ethanol has become almost clear as seen in the right segment of Figure 1(d) because all the nanocrystals have settled at the bottom. In contrast, the color of the dispersion in ethanol with ethyl cellulose remains black, indicating the beneficial role played by ethyl cellulose for producing a stable ink.

Figure 2 shows the SEM images of the as-prepared CZTSe films with or without ethyl cellulose after the sulfurization treatment at 480 and 570 °C. The morphology of the CZTSSe film with the use of ethyl cellulose after sulfurization at 480 °C in Figure 2(a) shows a clear feature of grain growth consisting of most crystallite grains in comparison to the film obtained without using ethyl cellulose that contains only agglomerated

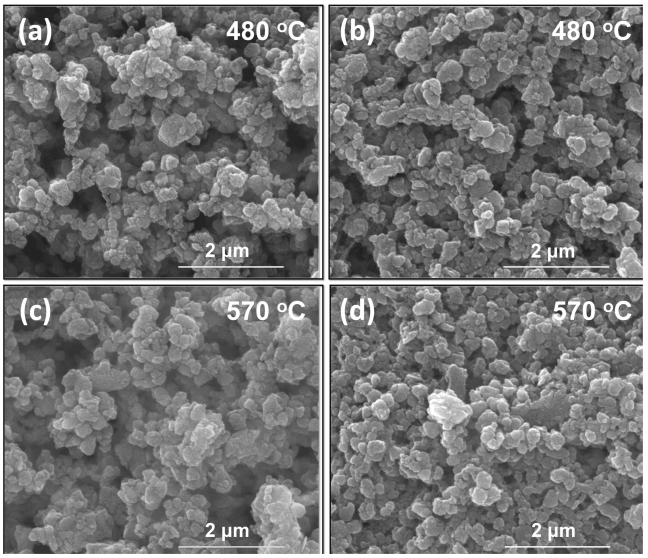

Figure 2. Plane view SEM images of CZTSe nanocrystals (a) with ethyl cellulose and (b) without ethyl cellulose after sulfurization at 480 °C. Plane view SEM images of CZTSe nanocrystals (c) with ethyl cellulose and (d) without ethyl cellulose after sulfurization at 570 °C.

particles as shown in Figure 2(b). Besides, the film using ethyl cellulose shows an enlarged grain size of 300–400 nm, as compared to the as-synthesized nanocrystals of 20 nm. Such induced grain growth at a low temperature of 480 °C for the film with the aid of ethyl cellulose could be attributed to the bridging together of the CZTSe nanocrystals by the polymer, leading to the precursor film with a higher packing density beneficial for the grain growth. In addition, the morphology of the film with ethyl cellulose after sulfurization at 570 °C in Figure 2(c) shows a denser microstructure of more crystallite grains along with the shrinkage of the pores than that at 480 °C. However, the microstructure of the film without ethyl cellulose after sulfurization at 570 °C in Figure 2(d) remains, consisting of most agglomerated particles instead of crystallite grains, further indicating that the evolution of grain is delayed due to the lack of ethyl cellulose.

In order to further understand the role of ethyl cellulose during the sulfurization treatment, a TGA experiment was carried out. Figure 3(a) shows the weight loss of the ethyl cellulose with temperature. As shown, the first decomposition of ethyl cellulose begins at about 150 °C, the second weight loss occurs at about 300 °C, and <1% weight of ethyl cellulose remains when the temperature is above 410 °C. This indicates that ethyl cellulose possesses the inherent properties of low ash and easy removal, which is suitable for the additive binder in the ink. However, it has been reported that the existence of a large amount of residual amorphous carbon layer at the bottom interface between Mo and $CuInSe_2$ (CIS) causes a negative effect on the device performance while adding the polymer as a viscosity controlling agent in the typical metal salts ink to prepare CIS absorbent films.[16] Such problems can be understood by considering that the evaporation path of ethyl cellulose after the heat treatment may be hindered by the upper dense layer with the early formation of CIS crystallite film, which results in a double-layer structure consisting of the incomplete removal of ethyl cellulose left at the bottom of the resulting film and the crystallite film at the top. As compared to the film prepared by the typical metal salts ink, our film prepared by nanocrystal-based ink with the ethyl cellulose

dx.doi.org/10.1021/sc400465m | ACS Sustainable Chem. Eng. 2014, 2, 561–568

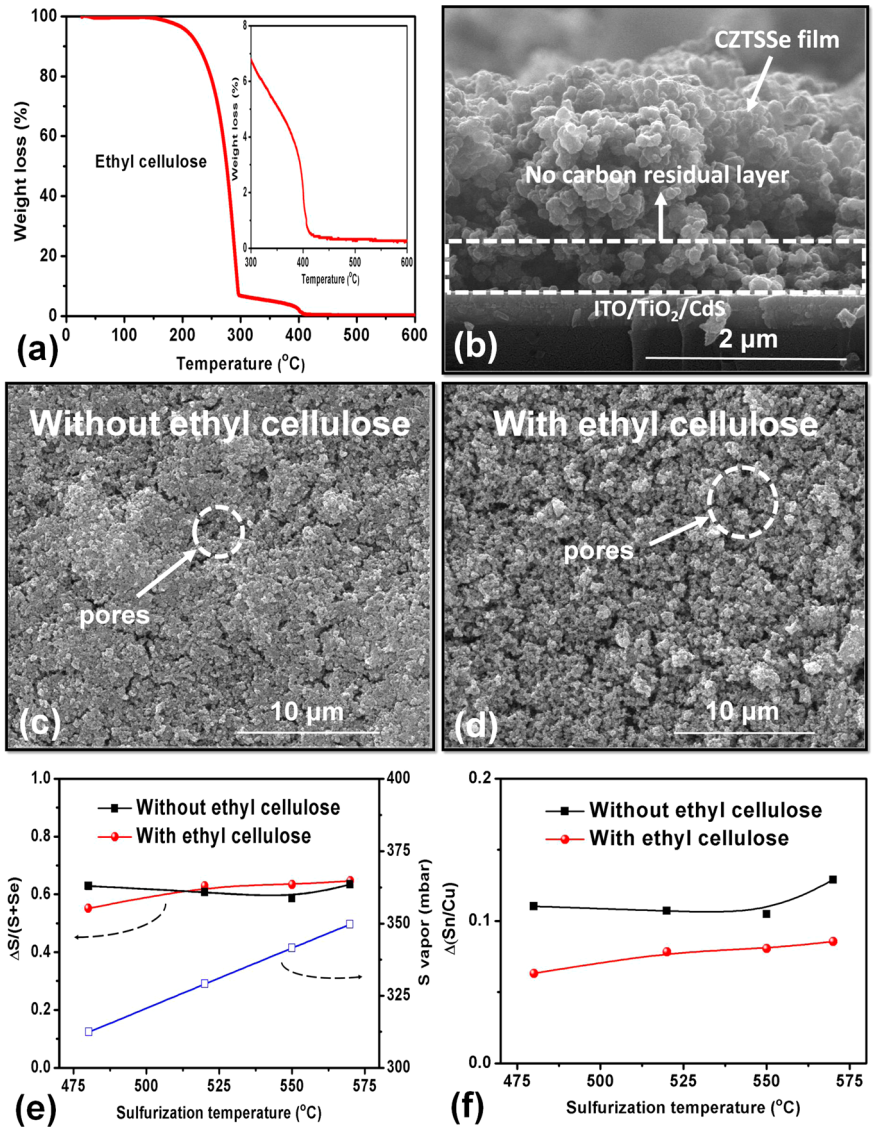

Figure 3. (a) TGA plots of ethyl cellulose and (b) cross-sectional SEM images of CZTSe nanocrystals with ethyl cellulose after sulfurization at 480 °C. Low magnification plane view SEM images of CZTSe nanocrystals (c) without ethyl cellulose and (d) with ethyl cellulose after sulfurization at 480 °C. The change in the compositional ratios of (e) S/(S+Se) and (f) Sn/Cu in the CZTSe nanocrystals as a function of sulfurization temperature.

additive shows a single-layer structure without a residual carbon layer at the interface between CZTSSe and CdS, as shown in Figure 3(b), which indicates all the carbon out of ethyl cellulose could be effectively removed through the existence of micropores between the nanocrystals. Direct evidence can be found in Figure 3(c), obtained with our nanocrystal ink without ethyl cellulose after sulfurization at 480 °C, showing the microstructure consisting of micropores. In addition, the film prepared by our nanocrystal ink with ethyl cellulose after sulfurization at 480 °C (Figure 3(d)) shows that more micropores in the film are created with the volume shrinkage of the precursor film while the ethyl cellulose is evaporated out of the film.

Furthermore, the EDS analysis, as shown in Figure 3(e), indicates the amount of S doped into the film (or the change in the compositional ratios of S/(S+Se)) without and with ethyl cellulose as a function of sulfurization temperature. The sulfurizaiton process was carried out by placing the samples with 2 mg of sulfur powder in a graphite box with a volume of 6.25 cm^3 under argon flow. The approximate pressure of S vapor during heat treatment as a function of temperature is also shown in Figure 3(e), all of which are higher than the required value to stabilize the formation of CZTS.[17] Although the pressure of S vapor increases with temperature, the observation of a nearly constant ratio of the change of S/(S+Se) around 0.6 in a large range of 480 to 570 °C would suggest that the amount of S doped into the CZTSe can be controlled during the sulfurization process. On the other hand, it can be found that the amount of S doped in the CZTSSe films using ethyl cellulose after sulfurization at 480 °C are lower than that without using ethyl cellulose because the potential existence of minor ethyl cellulose after sulfurization at 480 °C could retard the diffusion of S into the film. On the other hand, the amounts of S doped into the CZTSSe films using ethyl cellulose after sulfurization above about 520 °C are higher than that found using ethanol. This can be attributed to the increase in the number of micropores caused by the evaporation of ethyl cellulose binder. When there are more micropores in the film, a high amount of the S element can be easily doped into the film

dx.doi.org/10.1021/sc400465m | ACS Sustainable Chem. Eng. 2014, 2, 561−568

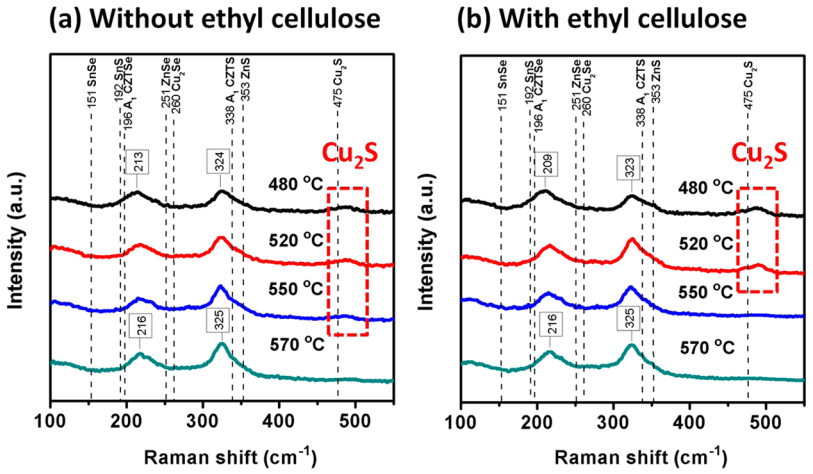

Figure 4. Raman spectroscopic analyses of the CZTSSe films fabricated with the CZTSe nanocrystals (a) without ethyl cellulose and (b) with ethyl cellulose as a function of sulfurization temperature. Raman peak locations of the compounds can be found in the literature.[6a,18,23]

through the micropores. The following reaction refers to such a doping path by replacing Se in CZTSe by S in the sulfurization

$$Cu_2ZnSnSe_4(s) + 2S_2(g) \rightarrow Cu_2ZnSnS_4(s) + 2Se_2(g)$$

Additionally, the role played by ethyl cellulose on the film quality during the grain growth process was further investigated and understood via the compositional change. In Figure 3(f), the EDS analysis indicates the compositional change in the Sn/Cu ratio as a function of the sulfurization temperature for the films with or without ethyl cellulose. The film without ethyl cellulose shows significant variations of the change in Sn/Cu ratio, while that with ethyl cellulose shows minor variations, indicating that ethyl cellulose can suppress the loss of Sn. Nevertheless, in order to understand the reaction pathway associated with the loss of Sn during the grain growth process, Raman spectroscopy was utilized for characterizing the CZTSSe film after the sulfurization. It is known that the major Raman peaks of pure CZTSe at 196 cm^{-1} and pure CZTS at 338 cm^{-1} are attributed to the A_1 anion vibration mode of the lattice, which corresponds to the vibration of Se (and S) relative to the fixed surrounding atoms. Such a variation in the major A_1 mode vibration with increasing ratio of Se to S leads to Raman shifts toward a smaller wavenumber while Se atoms are incorporated into CZTS at different levels. A bimodal behavior with major peaks shifting to the location between 196 and 338 cm^{-1} is usually observed.[18] Figure 4(a) (and (b)) shows the Raman analyses of devices obtained without (and with) using ethyl cellulose as a function of sulfurization temperature from 480 to 570 °C. As shown, shifting of two major peaks occurs, from 213 cm^{-1} (209 cm^{-1}) and 324 cm^{-1}(323 cm^{-1}) to 216 cm^{-1} (216 cm^{-1}) and 325 cm^{-1}(325 cm^{-1}), which are attributed to the change in the lattice vibrations on incorporating S into CZTSe. Besides, the XRD analysis of the CZTSSe devices with and without ethyl cellulose after sulfurization at 550 °C, as shown in Figure 5, indicates that the three main diffraction peaks of CZTSe also shift to higher angles due to the replacement of larger Se (0.198 nm) by smaller S (0.184 nm) during the sulfurizaiton process, which is consistent with the peaks shifts in the Raman analysis. These results are consistent with previous studies, showing the shifts in the XRD peaks and in the two Raman peaks of CZTSSe with the ratio of S/(S+Se) (210 and 329 cm^{-1} for S/(S+Se) = 0.4).[6a]

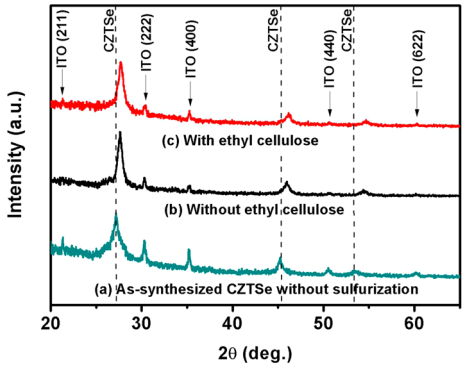

Figure 5. XRD patterns of (a) as-prepared CZTSe nanocrystals and CZTSe nanocrystals (b) without ethyl cellulose and (c) with ethyl cellulose after the sulfurization at 550 °C on a superstrate-type substrate of CdS/TiO_2/ITO/soda-lime glass.

However, a weak peak at 490 cm^{-1} corresponding to Cu_2S in the Raman spectrum of Figure 4(a), which cannot be detected by XRD, is found from the sulfurization temperature of 480 to 550 °C, which then disappeared after 570 °C. This indicates that a Cu_2S secondary phase forms in the film when no ethyl cellulose is used, and it exists during the grain growth process until the sulfurization temperature of 570 °C is reached. On the other hand, Figure 4(b) reveals that the 490 cm^{-1} peak corresponding to Cu_2S disappeared after the sulfurization temperature of 550 °C when ethyl cellulose is used. This finding is similar to Mainz et al.'s work[19] associated with the selenization process of CZTS nanocrystals that tend to form copper selenide by an initial intermediate separation of the cations at the surface, followed by the diffusion of Zn and Sn to form CZTSSe. As a result, the lower loss of Sn from the film with ethyl cellulose than that without ethyl cellulose, as recognized from Figure 3(f), can be explained to be due to a high packing density of the film to facilitate the diffusion of Zn and Sn to convert into CZTSSe. On the contrary, the film without ethyl cellulose is more prone to the evaporation of the Sn(S,Se) gas phase before compiling together, leading to a large amount of Sn loss from the film. Once the loss of Sn is too large, not only can the desirable composition of CZTSSe with the Cu-poor and Zn-rich condition not be realized but also the removal of the unwanted $Cu_2(S,Se)$ becomes difficult. No

dx.doi.org/10.1021/sc400465m | ACS Sustainable Chem. Eng. 2014, 2, 561−568

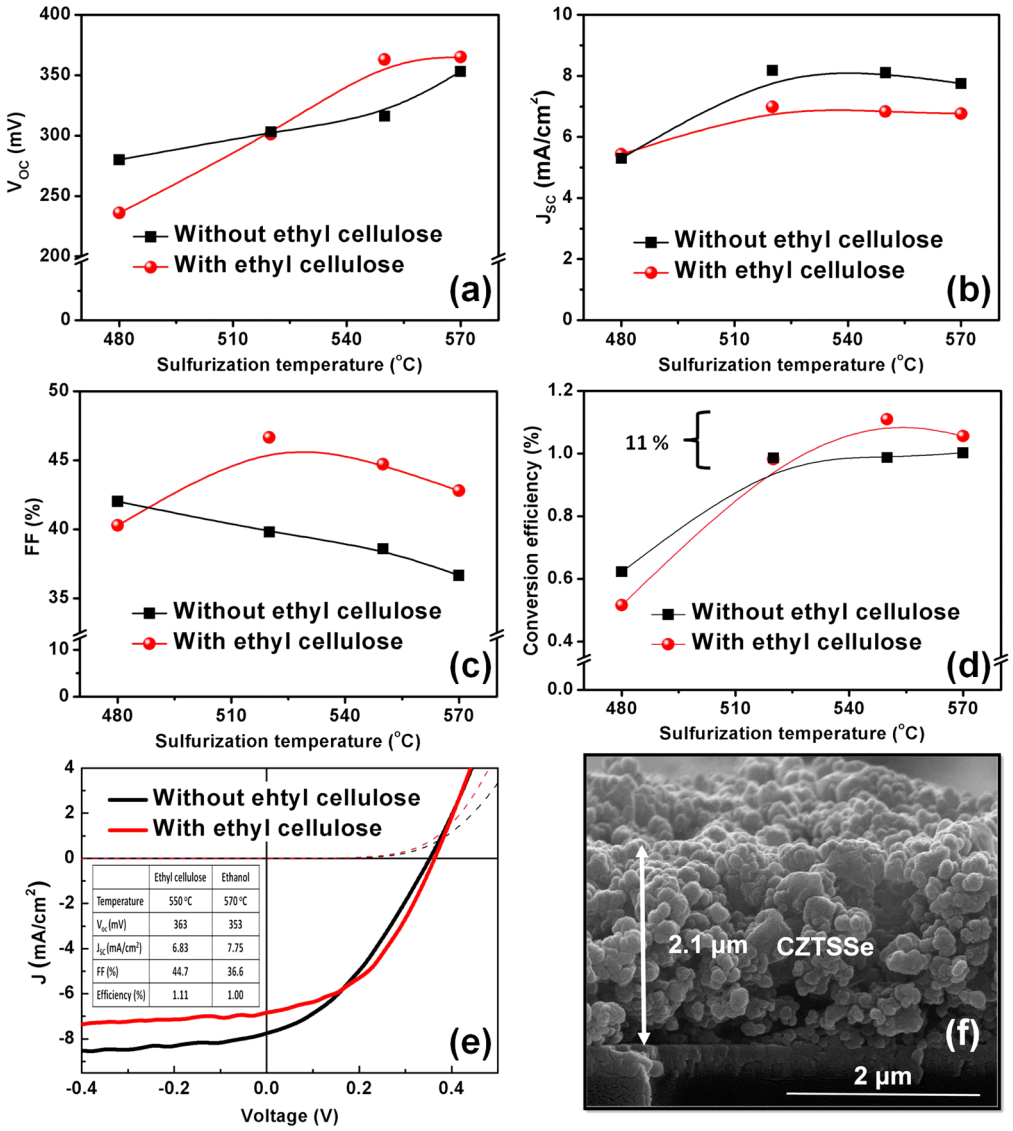

Figure 6. (a) V_{oc} of CZTSe nanocrystals with and without ethyl cellulose as a function of sulfurization temperature. (b) J_{sc} of CZTSe nanocrystals with and without ethyl cellulose as a function of sulfurization temperature. (c) FF of CZTSe nanocrystals with and without ethyl cellulose as a function of sulfurization temperature. (d) Conversion efficiency of CZTSe nanocrystals with and without ethyl cellulose as a function of sulfurization temperature. (e) J–V characteristics of the CZTSSe solar device with ethyl cellulose after sulfurization at 550 °C as marked by the red line and without ethyl cellulose after sulfurization at 570 °C as marked by the black line. The dashed lines correspond to the dark J–V curves. (f) Cross-sectional SEM image of CZTSe nanocrystals with ethyl cellulose after sulfurization at 550 °C.

detectable Raman peak of Zn(S,Se) may be attributed to the removal of Zn-rich compounds during the HCl etching process.[14]

In order to investigate the effectiveness of our route, the conversion efficiencies of CZTSSe solar devices prepared with the CZTSe nanocrystals with and without ethyl cellulose as a function of sulfurization temperature were evaluated. With increasing sulfurization temperature, not only the V_{oc} in Figure 6(a) but also J_{sc} in Figure 6(b) for the devices with and without ethyl cellulose can be raised. Such enhancement of V_{oc} and J_{sc} can be attributed to the reduced defects of CZTSSe during the grain growth process.

On the other hand, it is worth noting that Figure 6(c) shows that the values of FF for the films without ethyl cellulose decrease with increasing sulfurization temperature, but those with ethyl cellulose are much higher than those without ethyl cellulose at higher temperature. It can be explained that the ethyl cellulose additive in the CZTSSe film could not only effectively improve the film quality by promoting the grain growth as suggested by Figure 2(a) but also suppress the Cu_2S phase by mitigating the loss of Sn as explained by Figure 4(b). Furthermore, as compared to the previous reports showing low FF (~35%) with ethyl cellulose,[16] our device using ethyl cellulose with a higher FF (>40%) may be attributed to the complete removal of ethyl cellulose as shown in Figure 3(b).[20] As a result, it is believed that the ethyl cellulose additive in the nanocrystal-based ink would play a crucial role in tuning the CZTSSe film quality during the sulfurization treatment.

Figure 6(d) illustrates the conversion efficiency of solar devices with and without using ethyl cellulose as a function of sulfurization temperature. It shows that the double increase in the conversion efficiency can be achieved by increasing the temperature from 480 to 570 °C for both cases with and without ethyl cellulose, demonstrating that the modification of

dx.doi.org/10.1021/sc400465m | ACS Sustainable Chem. Eng. 2014, 2, 561−568

Table 1. Reported Efficiencies of $Cu_2ZnSn(S,Se)_4$ Nanocrystal-Based Absorbers

device structure	solvent	V_{oc} (mV)	J_{sc} (mAcm^{-2})	FF (%)	eff. (%)	ref
glass/Au/CZTS/CdS/ZnO/ITO	toluene	321	1.95	37.0	0.23	7
glass/Mo/CZTSSe/CdS/ZnO/ITO	toluene	210	11.5	33.1	0.80	9
glass/Mo/CZTSSe/CdS/ZnO/ITO	hexanethiol	420	30.4	52.7	6.73	10
glass/Mo/CZTSSe/CdS/ZnO/ITO	hexanethiol	451	29.0	64.9	8.50	24
glass/ITO/TiO_2/CdS/CZTSSe/Au	ethanol	353	7.75	36.6	1.00	this study
glass/ITO/TiO_2/CdS/CZTSSe/Au	EC[a]	363	6.83	44.7	1.11	this study

[a]EC refers to ethyl cellulose.

CZTSe nanocrystals by sulfurization treatment is applicable for promoting the quality of CZTSSe film. Besides, the efficiency of the device with ethyl cellulose is higher than that without ethyl cellulose after the sulfurization at 520 °C, which can be attributed to the removal of ethyl cellulose from the film. Figure 6(e) shows that our preliminary conversion efficiency of 1.11% with a V_{oc} of 363 mV, J_{sc} of 6.83 mAcm^{-2}, and FF of 44.72% has been achieved by using CZTSe nanocrystals and the ethyl cellulose binder after the sulfurization process at 550 °C, compared to an efficiency of 1.00% with a V_{oc} of 353 mV, J_{sc} of 7.75 mAcm^{-2}, and FF of 36.66% without using ethyl cellulose binder after the sulfurization process at 570 °C. Such an improvement of 11% in the conversion efficiency can be attributed to the removal of the unwanted Cu_2S secondary phase from the film at a lower sulfurization temperature of 550 °C by using ethyl cellulose.

Table 1 summarizes all reported efficiencies for CZTSSe fabricated by nanocrystal-based approaches. Compared to the previous work on CZTSSe fabricated by CZTS nanoparticles (without using malodorous hexanethiol) followed by a selenization process on the typical Mo substrate structure, our efficiency of 1% with a superstrate type substrate shows its promise with the comparable values of FF = 36.66% and V_{oc} = 353 mV. Besides, the increase in the conversion efficiency of the superstrate-type devices with the sulfurization temperature from 480 to 570 °C (Figure 6(d)) could suggest that the effect of the diffusion of CdS into the absorbent layer appear minor, even though the small amount of the diffusion of Cd into CZTSSe slightly increases with the sulfurizaiton temperature as shown in Figure S1 of the Supporting Information. It can explain the existence of the Cd_{Cu} defect via the diffusion of Cd into CZTSe to form the embedded n-type layer at the interface, which is beneficial for the device performance.[21] Furthermore, our fabrication method using CZTSe nanocrystals as the initial precursor also tends to mitigate the interdiffusion between CdS and the absorbent layer due to the relatively strong bonding between atoms in the crystallite structure, which differs from the previous post-annealing or co-evaporation approaches by using active metal or elemental gases as the initial precursors.[22] On the other hand, the diffusion of Ti and In into CZTSSe cannot be detected as shown, respectively, in Figures S2 and S3 of the Supporting Information. This indicates that TiO_2 film in the superstrate-type substrate is sufficient to block not only the diffusion of In from ITO into CdS but also the diffusion of Cd or S from CdS into ITO. These results of our device performance indicate that the superstrate type substrate has high potential to become a sustainable substrate for low-cost CZTSSe solar cells.

However, the high conversion efficiency of CZTSSe achieved by using hexanethiol, as given in Table 1, suggests that our initial device performance with a low short circuit current (7.75 mAcm^{-2} for ethanol and 6.83 mAcm^{-2} for ethyl cellulose) could be further raised by fabricating a robust film to improve the transport properties of electrons and holes. Figure 6(f) shows the cross-sectional microstructure of enlarged grains without tight packing caused by the removal process of ethyl cellulose during the sulfurization, so an increase in the recombination rate at the grain boundaries is highly possible to reduce the short circuit current. Secondarily, our CZTSSe absorbent thickness of 2 μm, as compared to 0.5 μm in the literature, would indicate that the possibility of more charge carrier traps in a thick film could cause the loss of the short circuit current. However, these problems can be addressed by improving the device-making processes, such as optimizing the ramping rate associated with the removal rate of ethyl cellulose in the heat treatment and the thickness of the CZTSSe films, to promote the carrier transport property. In addition, systematic studies on the ratio of S/Se and cation ratios of Zn/Sn and Cu/Zn+Sn to optimize the preferred defects in the CZTSSe film are currently underway in our group. We believe the route presented here would be a green, sustainable, and scalable approach for making low-cost efficient CZTSSe solar devices, as compared to the typical route involving toxic toluene or the stinky hexanethiol and harsh selenization process.

CONCLUSIONS

We have demonstrated a low-cost, environmentally friendly, scalable route for making CZTSSe films using CZTSe nanocrystals, synthesized by a hot injection approach, followed by a mild sulfurization process. With the addition of an ethyl cellulose binder into the ink, the evolution of CZTSe nanocrystals into CZTSSe film is promoted, while the loss of Sn during the evolution is suppressed, which is beneficial for increasing FF and manipulating the preferred composition. In addition, the solar devices with the CZTSSe film exhibit apparent improvements in V_{oc} and J_{sc}, suggesting this mild sulfurization process can offer device properties comparable to that achieved with the typical harsh selenization process.

ASSOCIATED CONTENT

Supporting Information

Content of Cd, Ti, and In in CZTSSe. This material is available free of charge via the Internet at http://pubs.acs.org.

AUTHOR INFORMATION

Corresponding Author

*Phone: (512) 471-1791. Fax: (512) 471-7681. E-mail: rmanth@mail.utexas.edu.

Notes

The authors declare no competing financial interest.

■ ACKNOWLEDGMENTS

Financial support by the Welch Foundation (Grant F-1254) is gratefully acknowledged. Silver paste provided by DuPont is also gratefully acknowledged. We thank Dr. Desiderio Kovar for discussion on ink preparation.

■ REFERENCES

(1) Hillhouse, H. W.; Beard, M. C. Solar cells from colloidal nanocrystals: Fundamentals, materials, devices, and economics. *Curr. Opin. Colloid Interface Sci.* **2009**, *14* (4), 245−259.

(2) Gur, I.; Fromer, N. A.; Geier, M. L.; Alivisatos, A. P. Air-stable all-inorganic nanocrystal solar cells processed from solution. *Science* **2005**, *310* (5747), 462−465.

(3) Panthani, M. G.; Akhavan, V.; Goodfellow, B.; Schmidtke, J. P.; Dunn, L.; Dodabalapur, A.; Barbara, P. F.; Korgel, B. A. Synthesis of $CuInS_2$, $CuInSe_2$, and $Cu(In_xGa_{1-x})Se_2$ (CIGS) nanocrystal "inks" for printable photovoltaics. *J. Am. Chem. Soc.* **2008**, *130* (49), 16770−16777.

(4) Ma, W.; Luther, J. M.; Zheng, H. M.; Wu, Y.; Alivisatos, A. P. Photovoltaic devices employing ternary PbS_xSe_{1-x} nanocrystals. *Nano Lett.* **2009**, *9* (4), 1699−1703.

(5) Wadia, C.; Alivisatos, A. P.; Kammen, D. M. Materials availability expands the opportunity for large-scale photovoltaics deployment. *Environ. Sci. Technol.* **2009**, *43* (6), 2072−2077.

(6) (a) Mitzi, D. B.; Gunawan, O.; Todorov, T. K.; Wang, K.; Guha, S. The path towards a high-performance solution-processed kesterite solar cell. *Sol. Energy Mater. Sol. Cells* **2011**, *95* (6), 1421−1436. (b) Ramsurn, H.; Gupta, R. B. Nanotechnology in solar and biofuels. *ACS Sustainable Chem. Eng.* **2013**, *1* (7), 779−797.

(7) Steinhagen, C.; Panthani, M. G.; Akhavan, V.; Goodfellow, B.; Koo, B.; Korgel, B. A. Synthesis of Cu_2ZnSnS_4 nanocrystals for use in low-cost photovoltaics. *J. Am. Chem. Soc.* **2009**, *131* (35), 12554−12555.

(8) Riha, S. C.; Parkinson, B. A.; Prieto, A. L. Compositionally tunable $Cu_2ZnSn(S_{1-x}Se_x)_4$ nanocrystals: Probing the effect of Se-inclusion in mixed chalcogenide thin films. *J. Am. Chem. Soc.* **2011**, *133* (39), 15272−15275.

(9) Guo, Q. J.; Hillhouse, H. W.; Agrawal, R. Synthesis of Cu_2ZnSnS_4 nanocrystal ink and its use for solar cells. *J. Am. Chem. Soc.* **2009**, *131* (33), 11672−11673.

(10) Guo, Q.; Ford, G. M.; Yang, W. C.; Walker, B. C.; Stach, E. A.; Hillhouse, H. W.; Agrawal, R. Fabrication of 7.2% efficient CZTSSe solar cells using CZTS nanocrystals. *J. Am. Chem. Soc.* **2010**, *132* (49), 17384−17386.

(11) Peter, L. M. Towards sustainable photovoltaics: The search for new materials. *Philos. Trans. R. Soc., A* **2011**, *369* (1942), 1840−1856.

(12) Shin, B.; Zhu, Y.; Bojarczuk, N. A.; Chey, S. J.; Guha, S. Control of an interfacial $MoSe_2$ layer in $Cu_2ZnSnSe_4$ thin film solar cells: 8.9% Power conversion efficiency with a TiN diffusion barrier. *Appl. Phys. Lett.* **2012**, *101* (5), 053903.

(13) Wang, C.-L.; Wang, C.-C.; Reeja-Jayan, B.; Manthiram, A. Low-cost, $Mo(S,Se)_2$-free superstrate-type solar cells fabricated with tunable band gap $Cu_2ZnSn(S_{1-x}Se_x)_4$ nanocrystal-based inks and the effect of sulfurization. *RSC Adv.* **2013**, *3* (43), 19946−19951.

(14) Fairbrother, A.; Garcia-Hemme, E.; Izquierdo-Roca, V.; Fontane, X.; Pulgarin-Agudelo, F. A.; Vigil-Galan, O.; Perez-Rodriguez, A.; Saucedo, E. Development of a selective chemical etch to improve the conversion efficiency of Zn-rich Cu_2ZnSnS_4 solar cells. *J. Am. Chem. Soc.* **2012**, *134* (19), 8018−8021.

(15) Ahn, S.; Jung, S.; Gwak, J.; Cho, A.; Shin, K.; Yoon, K.; Park, D.; Cheong, H.; Yun, J. H. Determination of band gap energy (E_g) of $Cu_2ZnSnSe_4$ thin films: On the discrepancies of reported band gap values. *Appl. Phys. Lett.* **2010**, *97* (2), 021905.

(16) (a) Yoon, H.; Woo, J. H.; Joshi, B.; Ra, Y. M.; Yoon, S. S.; Kim, H. Y.; Ahn, S.; Yun, J. H.; Gwak, J.; Yoon, K.; James, S. C. $CuInSe_2$ (CIS) thin film solar cells by electrostatic spray deposition. *J. Electrochem. Soc.* **2012**, *159* (4), H444−H449. (b) Ahn, S.; Kim, C.; Yun, J. H.; Gwak, J.; Jeong, S.; Ryu, B. H.; Yoon, K. $CuInSe_2$ (CIS) thin film solar cells by direct coating and selenization of solution precursors. *J. Phys. Chem. C* **2010**, *114* (17), 8108−8113.

(17) Scragg, J. J.; Ericson, T.; Kubart, T.; Edoff, M.; Platzer-Bjorkman, C. Chemical insights into the instability of Cu_2ZnSnS_4 films during annealing. *Chem. Mater.* **2011**, *23* (20), 4625−4633.

(18) Grossberg, M.; Krustok, J.; Raudoja, J.; Timmo, K.; Altosaar, M.; Raadik, T. Photoluminescence and Raman study of $Cu_2ZnSn(Se_xS_{1-x})_4$ monograins for photovoltaic applications. *Thin Solid Films* **2011**, *519* (21), 7403−7406.

(19) Mainz, R.; Walker, B. C.; Schmidt, S. S.; Zander, O.; Weber, A.; Rodriguez-Alvarez, H.; Just, J.; Klaus, M.; Agrawal, R.; Unold, T. Real-time observation of $Cu_2ZnSn(S,Se)_4$ solar cell absorber layer formation from nanoparticle precursors. *Phys. Chem. Chem. Phys.* **2013**, *15* (41), 18281−9.

(20) Lee, E.; Park, S. J.; Cho, J. W.; Gwak, J.; Oh, M. K.; Min, B. K. Nearly carbon-free printable CIGS thin films for solar cell applications. *Sol. Energy Mater. Sol. Cells* **2011**, *95* (10), 2928−2932.

(21) Maeda, T.; Nakamura, S.; Wada, T. First-principles study on Cd doping in Cu_2ZnSnS_4 and $Cu_2ZnSnSe_4$. *Jpn. J. Appl. Phys.* **2012**, *51*, 10NC11.

(22) (a) Nakada, T.; Okano, N.; Tanaka, Y.; Fukuda, H.; Kunioka, A. *Superstrate-Type $CuInSe_2$ Solar Cells with Chemically Deposited CdS Window Layers*. Proceedings of the 1st World Conference on Photovoltaic Energy Conversion, Hawaii, 1994, pp 95−98. (b) Ikeda, S.; Kamai, R.; Yagi, T. Y.; Matsumura, M. Electrochemical synthesis of $CuIn(Se,S)_2$ layer for thin-film solar cell with a superstrate configuration. *J. Electrochem. Soc.* **2010**, *157* (1), B99−B103.

(23) (a) Fernandes, P. A.; Salome, P. M. P.; da Cunha, A. F. Study of polycrystalline Cu_2ZnSnS_4 films by Raman scattering. *J. Alloy. Compd.* **2011**, *509* (28), 7600−7606. (b) Salome, P. M. P.; Fernandes, P. A.; da Cunha, A. F. Morphological and structural characterization of $Cu_2ZnSnSe_4$ thin films grown by selenization of elemental precursor layers. *Thin Solid Films* **2009**, *517* (7), 2531−2534. (c) Chandrasekhar, H. R.; Humphreys, R. G.; Zwick, U.; Cardona, M. Infrared and Raman spectra of the IV−VI compounds SnS and SnSe. *Phys. Rev. B* **1977**, *15* (4), 2177−2183. (d) Ishii, M.; Shibata, K.; Nozaki, H. Anion distributions and phase transitions in $CuS_{1-x}Se_x(x = 0 - 1)$ studied by Raman spectroscopy. *J. Solid State Chem.* **1993**, *105* (2), 504−511.

(24) Cao, Y. Y.; Denny, M. S.; Caspar, J. V.; Farneth, W. E.; Guo, Q. J.; Ionkin, A. S.; Johnson, L. K.; Lu, M. J.; Malajovich, I.; Radu, D.; Rosenfeld, H. D.; Choudhury, K. R.; Wu, W. High-efficiency solution-processed $Cu_2ZnSn(S,Se)_4$ thin-film solar cells prepared from binary and ternary nanoparticles. *J. Am. Chem. Soc.* **2012**, *134* (38), 15644−15647.